TISSUE ENGINEERING: Part A
Volume 16, Number 8, 2010

DOI: 10.1089/ten.tea.2009.0697

Early Stages of *In Situ* Bladder Regeneration in a Rodent Model

David Burmeister, B.S.,[1,2] Tamer AbouShwareb, M.D., Ph.D.,[1,3] Josh Tan, M.S.,[4] Kerry Link, M.D.,[4] Karl-Erik Andersson, M.D., Ph.D.,[1,2,3] and George Christ, Ph.D.[1,2,3]

Surgical removal of ≈70% of the bladder (subtotal cystectomy [STC]) was used as a model system to gain insight into the normal regenerative process in adult mammals *in vivo*. Female F344 rats underwent STC, and at 2, 4, and 8 weeks post-STC, bladder regeneration was monitored via microcomputed tomography scans, urodynamic (bladder function studies) pharmacologic studies, and immunohistochemistry. Computed tomography imaging revealed a time-dependent increase in bladder size at 2, 4, and 8 weeks post-STC, which positively correlated with restoration of bladder function. Bladders emptied completely at all time points studied. The maximal contractile response to pharmacological activation and electrical field stimulation increased over time in isolated tissue strips from regenerating bladders, but remained lower at all time points compared with strips from age-matched control bladders. Immunostaining of the bladder wall of STC rats suggested a role for progenitor cells and cellular proliferation in the regenerative response. Immunostaining and the presence of electrical field stimulation-induced contractile responses verified innervation of the regenerated bladder. These initial studies establish the utility of the present model system for studying *de novo* tissue regeneration *in vivo* and may provide guidance with respect to optimization of intrinsic regenerative capacity for clinical applications.

Introduction

In lower vertebrates such as the axolotl and the newt, regeneration of body parts, including limbs, jaws, tail, skin, spinal cord, brain, apex of the heart, and so on, has been well documented.[1,2] These amphibian kings of regeneration provide an excellent model for studying the true upper limit of regenerative capacity. However, adult mammals have a much more restricted repertoire for repair and functional replacement of damaged tissues/organ systems, which is generally thought to be largely restricted to epidermis, muscle, bone, and liver.[1] In this regard, a much less well-known example is the considerable regenerative capacity of the urinary bladder. The regenerative capacity of the bladder has been known for over a century, with an early report by Schwarz in 1891 describing a normal-sized bladder that had grown after subtotal cystectomy (STC; removal of a majority of the bladder) in dogs.[3] More recent studies in dogs have confirmed these initial observations,[4,5] and similar findings were made in rats, where STC without augmentation showed that bladder capacity (B_{cap}) returned to approximately half of the original size at 2 weeks postsurgery.[6,7] The capacity for the human bladder to regenerate has also been clearly demonstrated, starting with the work of Sisk and Neu in 1939, showing that organ growth ensued after removal of the entire bladder except 3 cm of the posterior bladder wall.[8] Studies by Bohne and Urwiller in the 1950s and Liang in the 1960s supported the conclusions by Sisk that bladder regeneration can occur in humans without the use of molds or scaffolds.[6,7,9] In this scenario, perhaps it is not surprising that after many years of preclinical work, Atala and colleagues have leveraged the regenerative capacity of the bladder and extended it to the clinic, utilizing a collagen/polyglycolic acid scaffold seeded with autologous cells implanted in patients with myelomeningocele.[10] Despite the unequivocal importance of this seminal clinical study, the implanted neobladders lacked the normal innervation required for micturition and thus provided a neoreservoir, rather than a functional bladder.

In light of the aforementioned considerations, and given the less than optimal alternative methods currently available for bladder repair in humans (e.g., detubularized bowel segments), it is clear that an improved understanding of the naturally occurring regenerative process in the urinary bladder would point toward novel and more effective regenerative therapies for urologic conditions. To this end, we have begun detailed investigations of the morphological and functional characteristics of bladder regeneration in adult

This work was presented in part in abstract form at the International Continence Society Meeting, San Francisco, California, 2009.
[1]Wake Forest Institute for Regenerative Medicine, Departments of [2]Physiology and Pharmacology and [3]Urology, and [4]Center for Biomolecular Imaging, Wake Forest University School of Medicine, Winston Salem, North Carolina.

rats following STC. The information gained from these studies undoubtedly has important implications for urologic tissue engineering, but likely also has much broader clinical applications as well, as these investigations also provide another important step toward improved understanding of organ regeneration in adult mammals.

Materials and Methods

Animals

A total of 78 female Fisher F344 rats weighing 170–200 g underwent STC (Fig. 1), with 9 animals dying postoperatively from urine leakage into the peritoneum (11.5% mortality rate) after STC. Additionally one rat was removed from the study because of the formation of stones, which was seen on computed tomography (CT) scans and confirmed when opening the bladder.

All protocols were approved by the Animal Care and Use Committee, Wake Forest University.

Trigone-sparing cystectomies

Animals were anesthetized with 2% isoflurane, and the abdominal wall was shaved. Pivodine–iodine was used as an antiseptic to decontaminate the surgical site. A low-midline abdominal incision was made, the bladder was identified, and the dome was delivered outside of the body. Two stay sutures were made on either side of the bladder, just above the ureteric orifices, using 6-0 polyglycolic acid. The dome portion of the bladder (60%–70%) was removed, leaving the trigone and ureters intact (trigone-sparing cystectomy). The remaining portion of the bladder was then sutured in a continuous fashion using one of the original stay sutures. The abdominal wall and skin were closed in two layers using 3-0 vicryl sutures. Animals were followed for up to 8 weeks post-STC.

CT imaging

CT scans of the animals were taken with a Siemens MicroCATII at 70 kV and 500 μA (BIN factor of 4, 200° rotation, 500 steps, 73 μm cuts), and the scans were centered on the bladder. Contrast medium (288 mg/mL iothalamate meglumine, diluted 1:3) was applied via transurethral catheterization and injected until bladder was full. All images were reconstructed using COBRA EXXIM version 4.9.52 and converted to DICOM images with Amira version 3.1. Analysis was done after transfer of images to TeraRecon Aquarius Workstation. Briefly, the entire image except the bladder was removed using the erase function. A bladder template was optimized with the following parameters: window width of 1116, window level of 657, and 11% opacity. Finally, the bladder circumference from the anterior view was selected with the freehand lasso tool, and the volume measurement tool was used for quantification.

Bladder catheter implantation

Catheters were implanted as described previously.[11,12] Briefly, rats were anesthetized with 2% isoflurane, and the bladder was dissected from ensuing adhesions caused by the previous surgery. The dome was delivered outside of the body as described earlier, a small incision was made, and a PE-50 intramedic polyethylene catheter (Becton-Dickinson) with cuff was inserted and anchored with a 5-0 purse string silk suture. The catheter was then tunneled subcutaneously, brought out through the nape of the animals, and held in place with cloth tape anchored to the skin via a 3-0 Vicryl

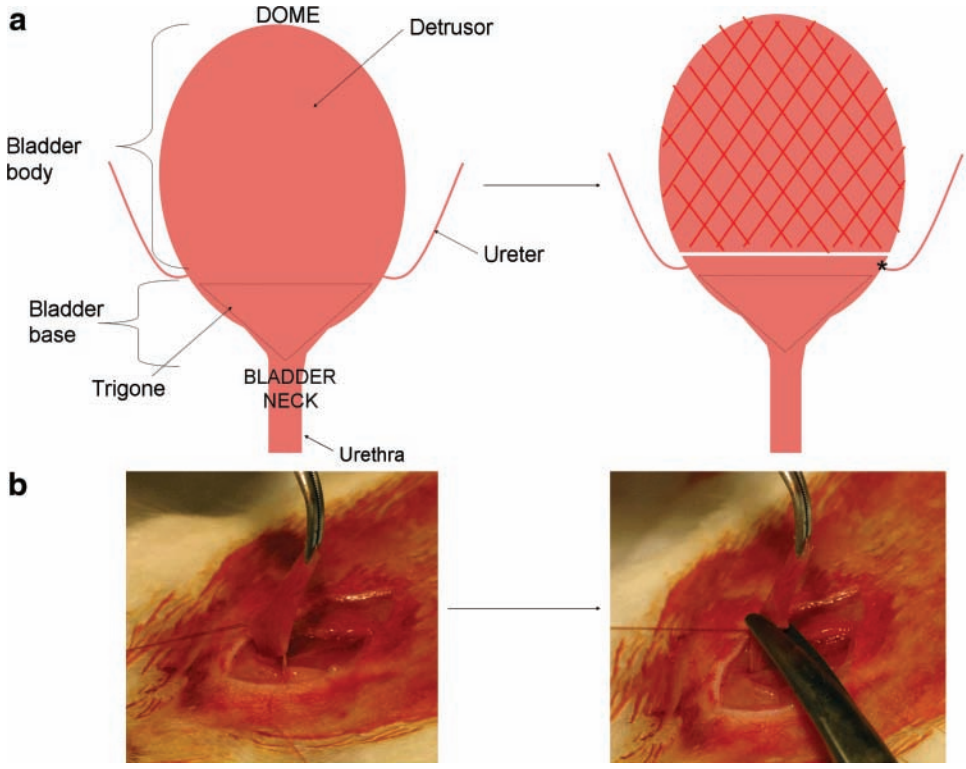

FIG. 1. Subtotal cystectomy (STC). (**a**) Cartoon depiction of STC. After dissection of the bladder, the bladder body is excised (~60%–70% of the total bladder), leaving the trigone and uretero–vesical junction (asterisk) intact. (**b**) Photographs of STC showing the bladder held in place with stay sutures before excision. Color images available online at www.liebertonline.com/ten.

suture. The abdominal wall and skin were closed in two layers with 3-0 vicryl sutures, and the free end of the catheter was thermally sealed.

Cystometric analysis

All cystometric studies were performed at 3 days after catheter implantation in conscious, freely moving rats as previously described.[11–13] Briefly, the bladder catheter was connected to a two-way valve that was, in turn, connected to a pressure transducer and an infusion pump. The pressure transducer was connected to an ETH 400 (CD Sciences) transducer amplifier and subsequently connected to a MacLab/8e (Analog Digital Instruments) data acquisition board. The pressure transducers and acquisition board were calibrated in cm H_2O before each experiment. Room-temperature saline was infused at a rate of 10 mL/h. Micturition volumes (MVs) were measured with a silicone-coated funnel leading into a collection tube that was connected to a force-displacement transducer. All analyses were conducted after a stable voiding pattern of at least 20 min was established. The following cystometric parameters were investigated: basal pressure (BP; lowest pressure between voids), micturition pressure (MP; the maximum pressure seen during a micturition cycle), threshold pressure (TP; pressure at which voiding is initiated), intermicturition pressure (mean bladder pressure between voids), B_{cap} (residual volume [RV] after last micturition plus amount of saline infused), MV (volume of expelled urine), RV ($B_{cap} - MV$), and bladder compliance (defined as $B_{cap}/[TP - BP]$).

In vitro *studies*

After cystometric analysis, animals were sacrificed with CO_2 inhalation and bilateral thoracotomy, and the bladders were harvested and immediately placed in ice-cold Krebs buffer. The bladders were cut into strips along the longitudinal axis. The strips were denuded of the urothelium and were attached to tissue holders at one end and force transducers at the other in an organ bath system (Danish Myo Technology) containing 15 mL of Krebs buffer aerated with 95% O_2/5% CO_2 at 37°C. Bladder strips were subjected to a resting tension of 2 g and allowed to stabilize for at least 60 min. They were then primed using 5 μM carbachol and subsequently 60 μM KCl. Contractions were recorded as changes in tension from baseline in response to both carbachol and electrical field stimulation (EFS). Carbachol dose–response curves were generated by adding increasing concentrations of carbachol at 0.5 log increments starting at 3 nM up to 100 μM. For EFS, strips were placed between two platinum electrodes in the organ chamber, and electrical pulses (0.1 ms pulse width, 20 V in the bath) were delivered, lasting 30 s at increasing frequencies (1, 2, 4, 8, 16, and 32 Hz), using an S88 stimulator (Grass Instruments). All tissue responses were normalized to grams of tissue weight.

Histological analysis

Bladders not subjected to pharmacological analysis were preserved for histology. After removal of the most superior part of the dome (~0.2 mm), bladders were fixed in 10% buffered formalin and processed. Serial 7 μm cross-sections were sliced along the upper part of the bladder wall (above the uretero–vesical junction). At least six sections were examined from the proximal and distal ends of the bladder. Slides cleared in xylene and rehydrated were used for staining. Staining with standard hematoxylin and eosin, and Gomori's one-step trichrome stain (Newcomer Supply catalog no. 9176A) was performed. For measurement of bladder wall thickness, at least five measurements were taken from three different sections of the bladder.

Immunohistochemistry was performed as follows: endogenous peroxidase activity was blocked with Dual Endogenous Enzyme Block (Dako; ref. no. S2003) for 10 min at room temperature, followed by 10 min incubation with Serum-Free Protein Block (Dako; ref. no×0909). Then samples were incubated with the following primary antibody dilutions/incubation times: c-kit (Santa Cruz; sc-168, rabbit polyclonal, 1:20 dilution) for 60 min, p63 (Lab Vision; no. MS-1081-P, mouse monoclonal, 1:200 dilution) for 30 min, PGP9.5 (Abcam; ab8189, mouse monoclonal, 1:20 dilution) for 60 min, and UP3 (Lifespan biosciences; LS-C40107, mouse monoclonal, 1:10 dilution) for 60 min. A heat-mediated antigen retrieval step was also used for PGP9.5 staining. Following primary antibody incubation, slides were treated with 30 min each of Biotinylated Universal Link and Streptavidin-HRP (Dako; ref. no. K0690). Finally, staining was completed with 5–10 min incubation with ImmPACT DAB (diaminobenzidine) from Vector Laboratories (catalog no. SK-4105). Immunohistochemistry probing proliferating cell nuclear antigen (PCNA) was performed similarly, without blocking endogenous peroxidase activity and without using diaminobenzidine as a chromogen. The primary antibody used was against PCNA (Abcam; ab29, mouse monoclonal, 1:3000 dilution) and the secondary antibody was conjugated with Texas Red (Vector Laboratories; catalog no. TI-2000).

Statistical analysis

Statistical evaluations were performed using GraphPad Prism software. For pharmacological analyses, individual response curves were placed in GraphPad software, and a mean curve was fit to the family of curves. The generated values were analyzed via one-way analysis of variances. One-way analysis of variances were also performed on cystometric evaluations and CT calculations. A p-value of less than 0.05 was considered significant. All results were expressed as the mean ± standard error of the mean.

Results

Rats that successfully recovered from surgery did not show any difference in weight gain compared with non-cystectomized animals (data not shown).

CT imaging

CT imaging of the bladder after STC revealed a progressive increase in bladder size. Figure 2 depicts subsequent images taken in two representative animals, and the average values for bladder volume at 1, 2, 4, 6, and 8 weeks post-STC as determined by TeraRecon analysis are graphed in Figure 3a. The morphology of the regenerated bladder was noted to change after regeneration, becoming more spherical in shape at 8 weeks post-STC when compared with the original more pear-shaped bladder.

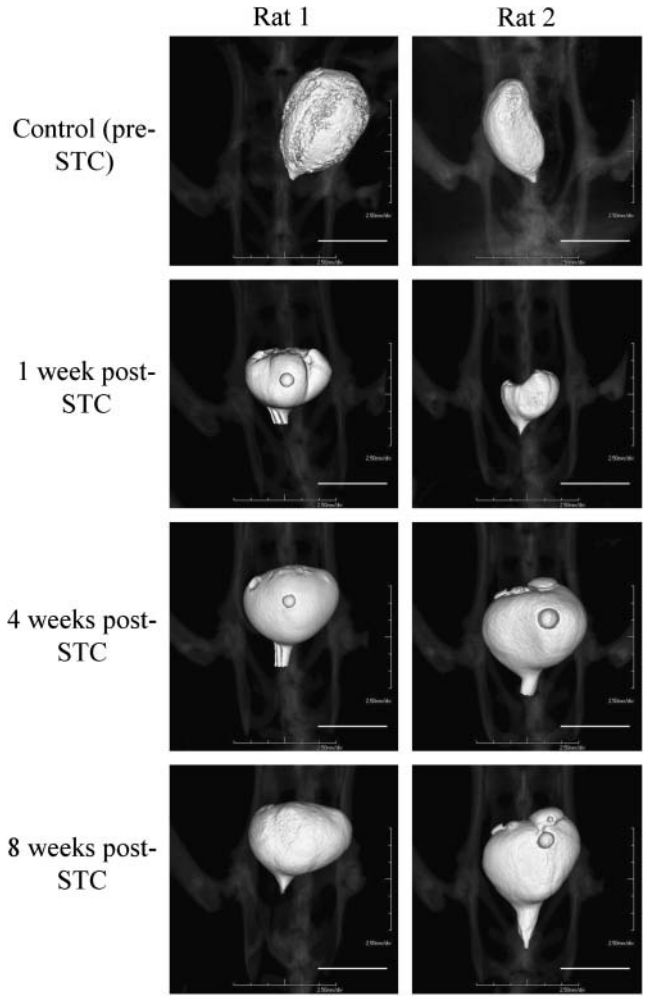

FIG. 2. Representative computed tomography (CT) images of the rat urinary bladder in two individual animals. Images are shown at 1, 4, and 8 weeks post-STC. Scale bars: 1 cm. All images are taken with a Siemens MicroCAT II, with reconstruction on TeraRecon software.

Cystometric analysis

All cystometric parameters from cystectomized and age-matched control animals are shown in Table 1. Age-matched controls were treated as one group because no age-dependent differences were noted in any of the cystometric parameters among the three time points (2, 4, and 8 weeks post-STC). Consistent with CT image analysis, cystometric studies also illustrated the progressive increase in bladder size (0.46 ± 0.03, 0.72 ± 0.05, and 0.85 ± 0.08 mL at 2, 4, and 8 weeks post-STC, respectively). Moreover, B_{cap} at the 8 weeks time point was not statistically different from controls (0.96 ± 0.05 mL).

MPs generated in animals at 2 weeks post-STC were reduced (30.5 ± 5.87 cm H_2O) compared with controls (49.24 ± 3.72 cm H_2O). However, MPs were not significantly different from controls at 4 weeks (38.15 ± 4.95 cm H_2O) and 8 weeks (37.31 ± 3.33 cm H_2O) post-STC. Importantly, at all time points the bladder was able to empty completely as evidenced by similar RVs between age-matched control and post-STC animals (Table 1). There was no significant difference in either the threshold or BP. In addition, statistical analysis also revealed significant differences in the calculated parameter (TP/MP). TP/MP nominally denotes the relationship between the pressure at which micturition is initiated relative to the maximal pressure at which micturition occurs. As indicated in Table 1, TP/MP was significantly different at all time points post-STC.

CT and cystometric regression

One of the goals of this initial investigation was to determine if noninvasive imaging could provide guidance regarding bladder regeneration and function. Figure 3a demonstrates that the rate of bladder volume increase is very comparable to that determined by urodynamic studies, which is evidenced by comparable linear regression slopes. Although the actual values of bladder volume may be lower than that obtained via functional methods, the progress of bladder regeneration can be illustrated, and the technique is consistent. Moreover, as illustrated in Figure 3b, there was a statistically significant positive correlation observed between MP determined by cystometric techniques and the bladder circumference determined by CT analysis ($r = 0.634$, $p < 0.05$). These data are consistent with the supposition that the observed increase in bladder size correlates well with the observed increase in bladder function.

In vitro *studies*

Steady-state concentration response curves were obtained for carbachol-induced contractile responses in bladder strips from both age-matched control and post-STC animals. Mean values for logistic parameter estimates are shown in Table 2, and the data are graphically depicted in Figure 4. In short, logistic analysis revealed a significant reduction in the calculated maximal steady state response (E_{max}) values in isolated detrusor strips from the regenerating bladder at all time points (Fig. 4). However, evidence for functional recovery over time was noted as, for example, the E_{max} at 8 weeks post-STC was significantly greater than that observed at both 2 and 4 weeks post-STC. As illustrated in Figure 4 and summarized in Table 2, there was no detectable difference in either pEC_{50} (the $-$log of the agonist concentration that results in 50% of the maximum response) or hill slope parameters among the groups.

The maximum contractions of regenerating detrusor smooth muscle strips induced by EFS was also significantly lower than native tissue at all frequencies tested, and the ratio of native responses to experimental responses was similar across all frequencies (Fig. 5). Moreover, there was again functional recovery in that responses generated in bladders at 8 weeks post-STC were greater than those at 2 weeks post-STC.

Histological analysis

The wall of regenerating bladders apparently retains the architecture of the native bladder. Consistent with this supposition, Figure 6 shows representative examples of hematoxylin and eosin staining of both native and 8-week regenerated bladder samples from the same animal. As illustrated, the urothelial, suburothelial, and smooth muscle layers are evident in the regenerating bladders. Similar staining of these layers was also seen with trichrome staining

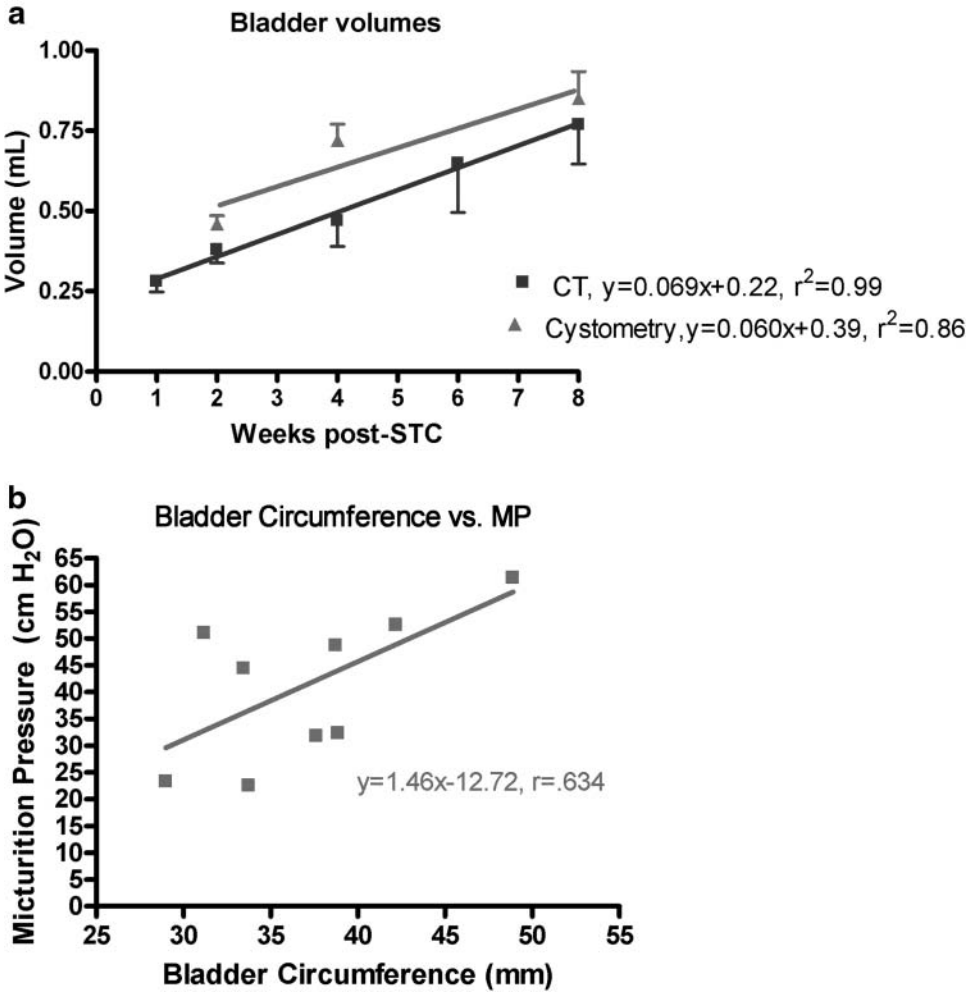

FIG. 3. Linear regression involving cystometric and imaging parameters. (**a**) Bladder volume averages for animals studied via cystometry (triangles) and CT imaging (squares). (**b**) Regressional analysis of micturition pressure (MP) determined by cystometry and anterior bladder circumference determined by Tera Recon CT image analysis. Only animals from the 4 and 8 weeks time points, with CT and cystometry data, were used ($n = 9$). A positive correlation was found between the two parameters ($r = 0.634$, $p < 0.05$).

(data not shown). Importantly, bladder wall thickness at the 8 weeks time point ($581.7 \pm 19.11\,\mu m$) was not significantly different from control bladders ($558.7 \pm 8.68\,\mu m$) as shown in Figure 6b.

To gain some preliminary insight into the mechanistic basis for bladder regeneration in this animal model, we compared fluorescent immunostaining with PCNA in post-STC and age-matched control bladder strips. As shown in Figure 7, there was an increased number of PCNA-positive proliferating cells in regenerating bladders at 2, 4, and 8 weeks post-STC. In another attempt to begin to characterize the proliferating cell population, immunohistochemical staining was performed for the presence of CD117 (c-kit)-positive cells in the bladder wall/detrusor muscle at all time points after

Table 1. Urodynamic Parameters as Determined by *In Vivo* Cystometry

	B_{cap} (mL)	MV (mL)	RV (mL)	BP (cm H_2O)	TP (cm H_2O)	MP (cm H_2O)	TP/MP
Controls, $n = 16$	0.96 ± 0.05	0.90 ± 0.05	0.05 ± 0.01	12.92 ± 0.89	28.14 ± 1.71	49.24 ± 3.72	0.59 ± 0.13
2 weeks, $n = 10$	$0.46 \pm 0.03^{a,b,c}$	$0.42 \pm 0.03^{a,b,c}$	0.05 ± 0.02	11.17 ± 2.48	22.36 ± 3.66	30.5 ± 5.87^{a}	0.75 ± 0.07^{a}
4 weeks, $n = 9$	0.72 ± 0.05^{a}	0.67 ± 0.07^{a}	0.06 ± 0.03	14.01 ± 2.64	27.08 ± 3.28	38.15 ± 4.95	0.72 ± 0.11^{a}
8 weeks, $n = 8$	0.85 ± 0.08	0.76 ± 0.06	0.09 ± 0.04	10.83 ± 1.18	25.92 ± 2.6	37.05 ± 3.36	0.7 ± 0.07^{a}

Age-matched controls revealed no differences and were subsequently grouped together as controls.
[a]Significant compared with controls.
[b]Significant compared with 8 weeks animals.
[c]Significant compared with 4 weeks animals ($p < 0.05$).
B_{cap}, bladder capacity; MV, micturition volume; RV, residual volume; BP, basal pressure; TP, threshold pressure; MP, micturition pressure.

Table 2. Parameters Obtained from Carbachol Dose–Response Curves

	E_{max} (g/g tissue)	Log [EC50] (log [carbachol])	Hill slope
Control, $n = 30$ strips, 20 animals	183.2 ± 5.97	-5.85 ± 0.25	1.34 ± 0.30
2 weeks, $n = 14$ strips, 10 animals	30.91 ± 4.49[a]	-5.61 ± 0.25	0.91 ± 0.44
4 weeks, $n = 15$ strips, 9 animals	35.94 ± 3.37[a]	-5.62 ± 0.15	1.33 ± 0.15
8 weeks, $n = 23$ strips, 12 animals	54.03 ± 5.36[a,b]	-6.05 ± 0.21	1.01 ± 0.46

[a] E_{max} at all time points is significantly lower than control ($p < 0.001$).
[b] E_{max} values at the 8 weeks time point is significantly higher than those found at 2 and 4 weeks post-STC ($p < 0.05$). There was no difference between groups for either the EC50 or the hill slope values.
STC, subtotal cystectomy; E_{max}, maximal effect; EC50, carbachol concentration producing 50% of the maximal response.

surgery. As shown in Figure 8, c-kit-positive staining was much more prominent in regenerating bladder strips at all time points post-STC. Additionally, in an attempt to evaluate the extent of innervation, immunohistochemistry against protein gene product PGP9.5 was performed. As illustrated, the presence of nerves in the regenerating bladder was clearly demonstrable including the presence of both nerve ganglia and bundles 4 weeks post-STC (Fig. 9). Finally, to evaluate the extent of regeneration of the bladder urothelial lining, staining was performed using antibodies to uroplakin 3. Once again, as illustrated, these studies revealed a mature urothelium as early as 1 week post-STC (Fig. 9).

Discussion

Chronic bladder disease can be the result of many pathological conditions (i.e., infections, congenital disorders, and inflammation), ultimately reducing bladder function and adversely affecting the quality of life. As noted in the Introduction section, currently available treatment options have both limited efficacy and untoward side effects.[14–19] To circumvent the side effects associated with these treatments, matrix grafts have recently been used. Animal studies with both bladder acellular matrix grafts and small intestinal submucosa have shown that urothelium, smooth muscle, nerves, and vasculature have the ability to infiltrate the graft. Atala and colleagues have even extended this to the clinic, utilizing a collagen/polyglycolic acid scaffold seeded with autologous cells implanted in patients with myelomeningocele.[10] Despite the importance of this seminal clinical study, the implanted neobladders lacked normal innervation required for micturition, thus limiting the functionality of the implanted construct. Moreover, this study was performed on otherwise healthy patients (young patients with spinal cord injuries), whereas older patients or those with compromised health (cancer, diabetes) generally have a far less regenerative capacity.[20–22] Because of the less than optimal methods currently provided for bladder repair, an improved understanding of the naturally occurring regenerative process would clearly help extend the applicability of this technology.

In this regard, Frederiksen *et al.* showed that after STC the newly formed detrusor had pharmacological properties similar to the supratrigonal region from which it had developed.[23] A later study by this group demonstrated that the nerves of the well-innervated regenerated bladder had originated from preexisting nerves in the detrusor.[24] Although these studies do provide some insight into the regeneration of the bladder following STC, the process remains not fully understood. To this end, we report herein our use of a rodent model to examine the early stages of *in situ* bladder regeneration that occurs following STC. The rationale for the use of the rodent model was twofold: (1) the overall similarity between the lower urinary tracts in rats and humans, and (2) the consistent evidence that bladder regeneration occurs in both.

Consistent with previous studies,[25,26] our current urodynamic investigations confirmed a rapid increase in size of the bladder following STC. Of importance is that, over the time frame of these investigations, the B_{cap} of the regenerating bladder did not exceed the value observed for that same animal prior to STC. The mean values for MP post-STC were decreased at 2 weeks (≈40%), but similar at 4 and 8 weeks (≈80% of control values in both cases) post-STC (Table 1). To our knowledge, this is the first demonstration of

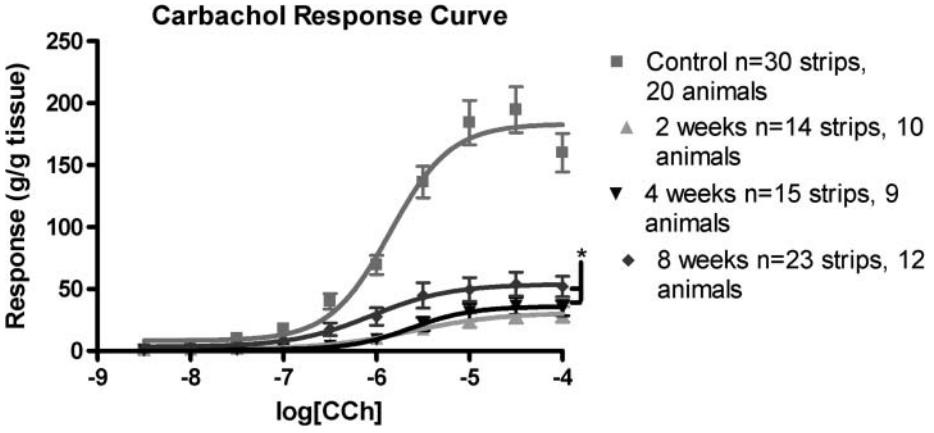

FIG. 4. Carbachol dose–response curves from both control animals and at 2, 4, and 8 weeks post-STC. Responses have been normalized to strip weight. Total area under the curve values were 312.8 for controls, 54.65 at 2 weeks, 61.86 at 4 weeks, and 119.7 at 8 weeks post-STC. Maximal steady state (*E_{max}) values for all STC animals are significantly lower than control tissue ($p < 0.001$). E_{max} values at 8 weeks post-STC are significantly higher than 2 and 4 weeks time points ($p < 0.05$).

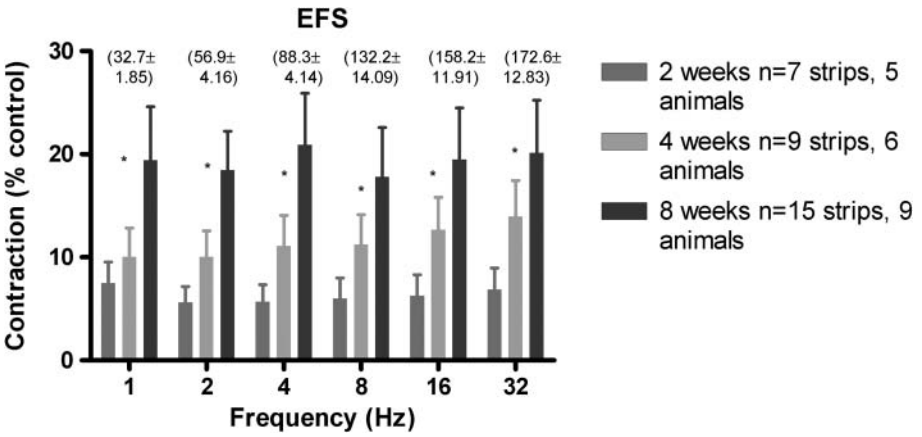

FIG. 5. Tissue responses to electrical field stimulation (EFS) for bladders at 2, 4, and 8 weeks post-STC. Responses have been normalized to strip weight and are shown as percent control. Values in parentheses are normalized responses for control tissue at each frequency. *All groups are different from each other as determined by one-way analysis of variance ($p < 0.001$).

in vivo pressure recovery following STC alone. Moreover, this functional recovery in MP is positively correlated with the increased bladder size detected using noninvasive micro-CT imaging techniques (Figs. 2 and 3). In the future, this latter observation may be of particular importance for monitoring the success of the regenerative process in patients. Interestingly, even in the presence of diminished MP, the bladder was able to empty completely (RV was the same at all time points). The precise reason for this observation is not clear, but may be related to, for example, a reduction in urethral outlet resistance. Certainly, this will be the subject of future investigation.

In addition, the observed functional recovery occurred despite the significant differences detected for the calculated parameter TP/MP at all time points post-STC. This finding is consistent with the presence of a perturbation in the relationship between the pressures required to initiate micturition (i.e., TP) relative to the maximal pressure generated during micturition (i.e., MP). Although the mechanistic basis for this observation in unknown, it does provide further evidence of the apparent physiological adaptability of the regenerated bladder, which is able to maintain normal bladder emptying despite the occurrence of such alterations in cystometric parameters, at least up to the 8 weeks time point. We believe that these observations, along with the changes in detrusor contractility described below, point toward to the plasticity/accommodation of the bladder regeneration process with respect to maintenance of bladder function post-STC.

Of note, these studies also documented a greatly reduced contractile response to carbachol (a muscarinic receptor

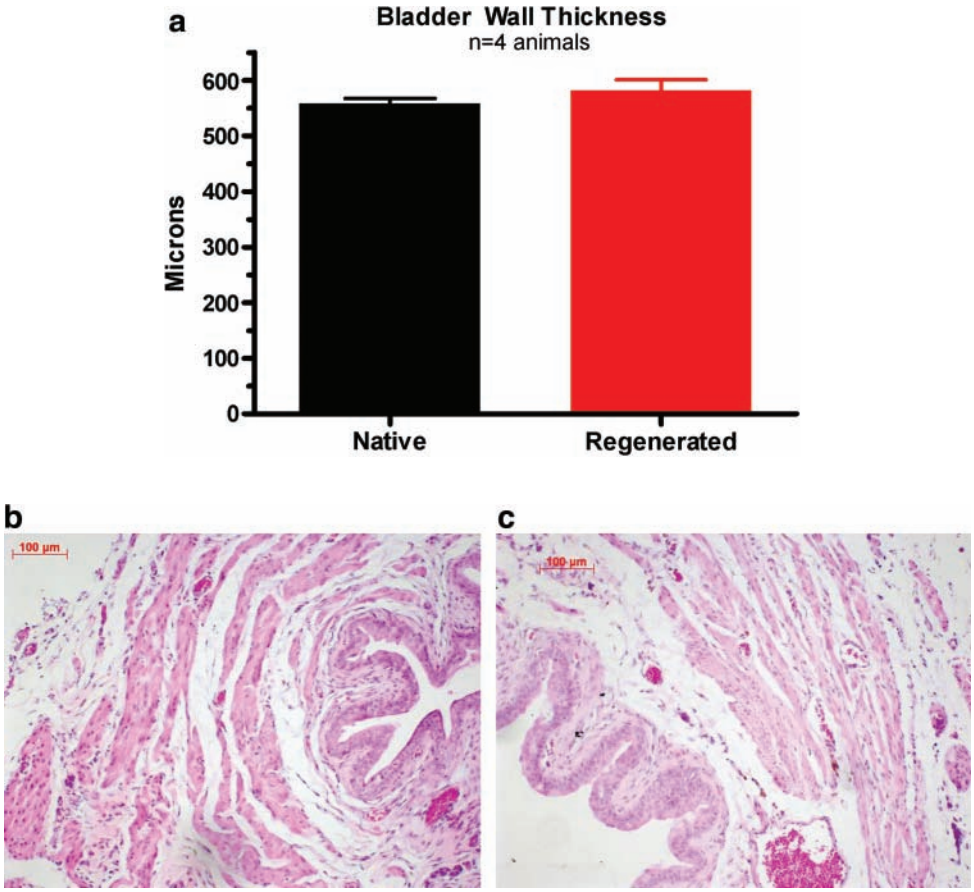

FIG. 6. Histological comparison between native and regenerated bladders at 8 weeks post-STC using hematoxylin and eosin staining. (**a**) Average bladder wall thickness of native and 8 weeks regenerated tissue. Values are mean ± standard error of the mean of five measurements of two sections from four animals in each group. Representative images of native tissue (**b**) and 8 weeks regenerated tissue (**c**) are shown at 10× magnification. Color images available online at www.liebertonline.com/ten.

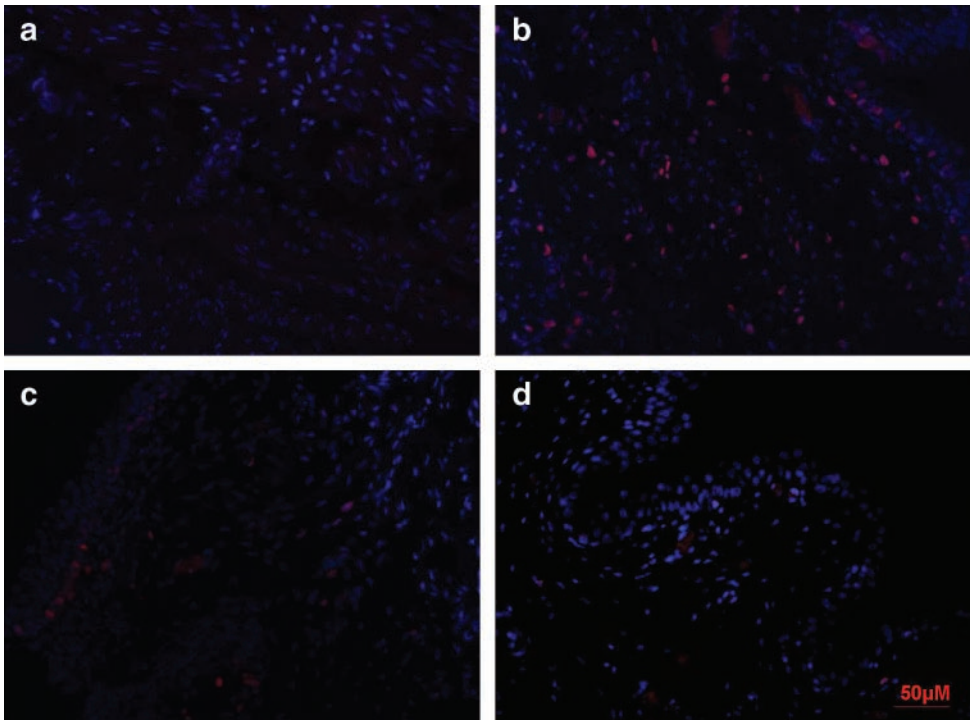

FIG. 7. Fluorescent immunostaining to proliferating cell nuclear antigen shows proliferating cells in the regenerating bladder at 2 weeks (**b**), 4 weeks (**c**), and 8 weeks (**d**) post-STC in greater abundance compared with control tissue (**a**). It is noticeable that the number of proliferating cells is decreasing over time, which is more evident at the 8 weeks time point when compared with the 2 weeks. Proliferating cell nuclear antigen staining is shown with Texas Red, and nuclei are stained with 4′,6-diamidino-2-phenylindole (blue). All images are shown at 40× magnification. Color images available online at www.liebertonline.com/ten.

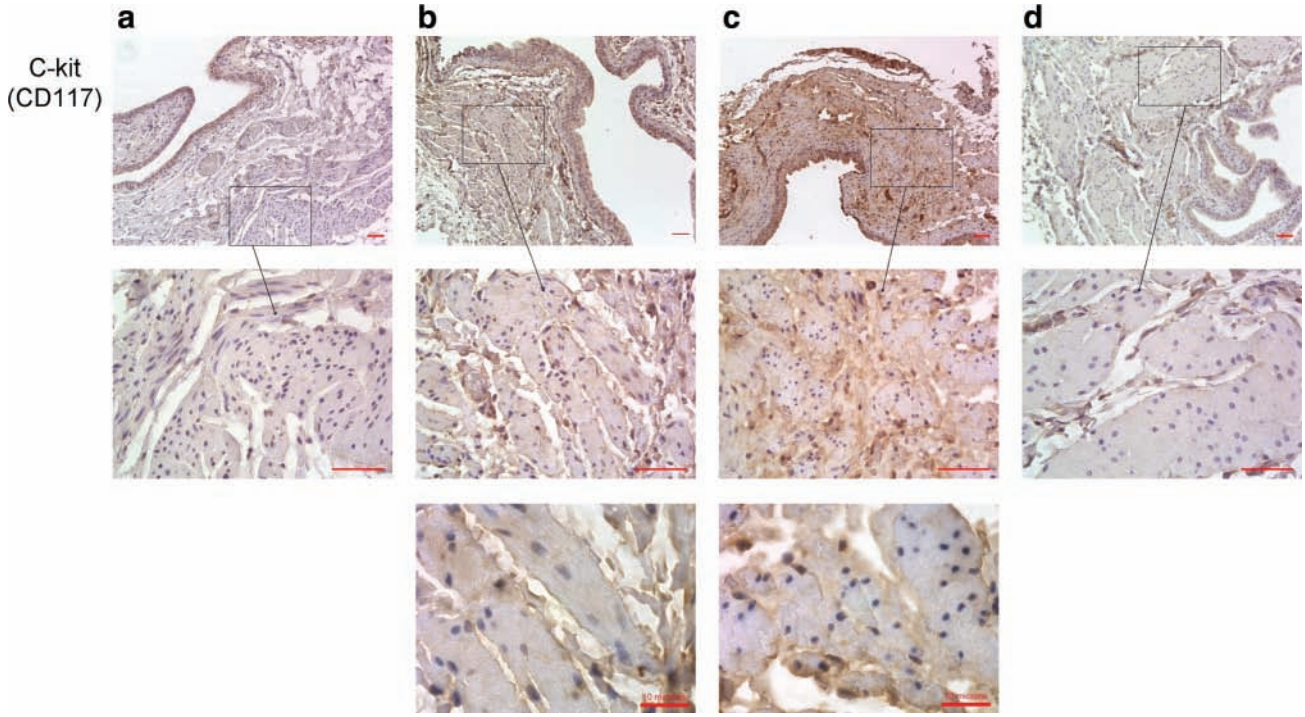

FIG. 8. Positive immunostaining for CD117 (c-kit)-positive cells in the smooth muscle during bladder regeneration. Staining is demonstrable in the detrusor at 2 weeks (Column **b**), 4 weeks (Column **c**), and to a lesser extent, 8 weeks (Column **d**) post-STC, but not prevalent in control tissue (Column **a**). All top images are shown at 20× magnification with scale bars of 50 μm, middle images are shown at 63× magnification with scale bars of 50 μM, and bottom 2 images are 100× with scale bars of 10 μM. Color images available online at www.liebertonline.com/ten.

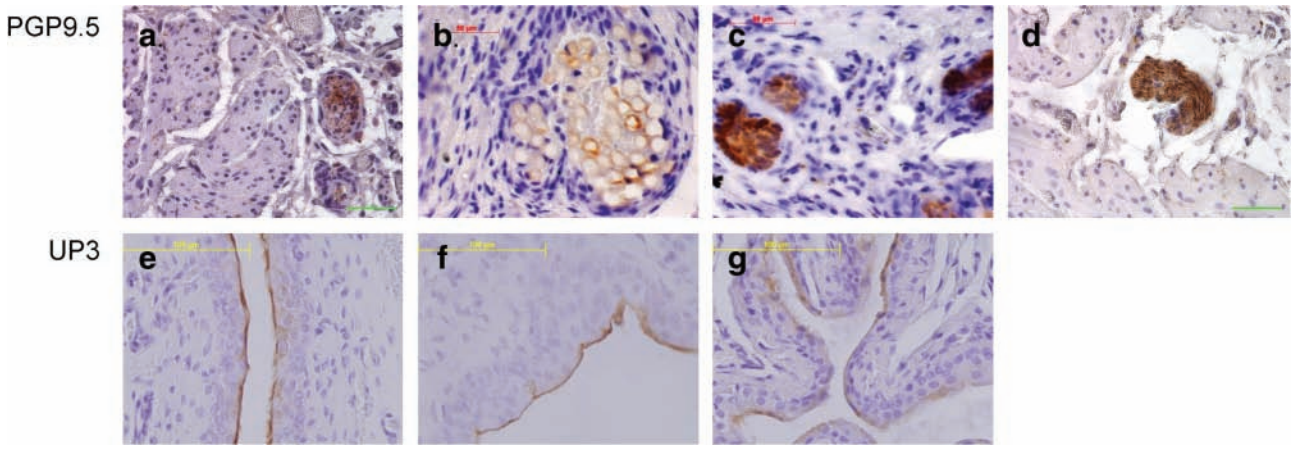

FIG. 9. Innervation of regenerated bladders is shown using immunohistochemistry to PGP9.5 at 2 weeks (**a**), 4 weeks (ganglia, **b**; nerve bundles, **c**) and 8 weeks (**d**) post-STC. Uroplakin (UP3) staining reveals a mature urothelium as early as 1 week post-STC (**f**), which is maintained 4 weeks post-STC (**g**), which closely resembles control tissue (**e**). All images are shown at 40× magnification. Color images available online at www.liebertonline.com/ten.

agonist), at all time points examined, albeit with a gradual improvement at 8 weeks post-STC (Table 2, Fig. 4). The observed decline in muscarinic contractility is consistent with an earlier study by Saito *et al.*[26] An even more marked reduction in detrusor contractility was observed in response to EFS (80%–90%; Fig. 5) As such, the decline in detrusor contractility is clearly much more pronounced than the initial decline in MP. The reason for this is unclear. Qualitatively, there was no difference in smooth muscle bundles (Fig. 6), and others have reported no change in smooth muscle actin content or the myosin/actin ratio.[27] Frederiksen *et al.* (2004) demonstrated that 15 weeks post-STC there was no difference in the contractile response to carbachol between controls and STC animals, and that a small contractile response remained after simultaneous adrenergic, muscarinic, and purinergic receptor blockade.[23] This led to the conclusion that the newly formed detrusor had pharmacological properties similar to the region from which it had developed (supratrigonal rim). It is important to keep in mind that Frederiksen *et al.* (2004) used transverse strips, whereas we have chosen longitudinally cut preparations. Thus, our results involving reduced carbachol contraction following STC could be explained by differing receptor populations, specifically those more closely related to the trigone and urethra (i.e., α-adrenergic).

As illustrated in Figure 6, the regenerating bladder had all layers characteristic of the native bladder. Specifically, a serosal layer was present, along with a mature urothelium and detrusor smooth muscle bundles. Importantly, proliferating cells were present in all layers of the bladder after STC, which indicates an important role of hyperplasia/cellular proliferation in the regenerative process (Fig. 7). Moreover, the abundance of proliferating cells was present in sections taken toward the distal end (dome) of the regenerating bladder, especially in terms of the urothelium. The logical implication of this finding is that the regenerative process involves an outgrowth from the distal end of the bladder (where the STC occurred). Moreover, it seems logical that there would be a diminution in the proliferative cellular response over the same time frame that the size of the regenerated bladder first approximates (e.g., at 4 weeks) and then achieves (e.g., at 8 weeks) the original bladder size in the same animal.

Associated with these regenerating smooth muscle bundles is a population of as yet unidentified stem/progenitor cells expressing CD117 (c-kit; Fig. 8). This observation is consistent with the supposition that stem/progenitor cells are involved in the proliferation of the detrusor smooth muscle in response to STC. Although the cell membrane expression revealed by our staining is in agreement with that previously reported for interstitial cell of cajal (ICC)-like cells in the bladder wall, the localization and morphology of the c-kit-positive cells in this study is distinct, possibly attributed to a novel function of c-kit-positive stem/progenitor cells in the regenerating urinary bladder.[28–32] In this regard, c-kit is a tyrosine kinase receptor whose endogenous ligand is a stem cell factor.[33] Although most often associated with hematopoietic stem cells, there is recent evidence that CD117-positive cells are the source of stem cells/progenitors in, for example, cardiac regeneration.[34–38] In this scenario, it is conceivable that the CD117-positive staining reported herein also identifies a bladder stem cell/progenitor capable of regenerating lost or damaged bladder tissue. This is the first suggestion of a bladder wall (detrusor) stem/progenitor cell *per se* that we are aware of. Further evaluation of this exciting hypothesis, as well as a more precise description of the identity of these cells, is of high priority for future investigations with this model.

In addition, the population of progenitor cells involved in urothelial turnover is also of interest, and several studies have explored the possibility of identifying urothelial stem cells.[39,40] We found uroplakin 3 staining as early as 1 week post-STC, indicating that the barrier function of the urothelium is maintained throughout bladder regeneration (Fig. 9). Our finding that the superficial cells of the urothelium are terminally differentiated at the earliest time point is, although important, not a surprising one. Normally, urothelial turnover is very low, but in response to injury, urothelial cells are known to rapidly proliferate.[41]

The presence of nerves in the newly formed bladder after STC was demonstrated functionally by the response to electrical stimulation of nerves (Fig. 5), and morphologically with PGP9.5 staining (Fig. 9). Evidence exists for the presence

of intramural ganglia in the female rat bladder, similar to what we observed in these studies.[42,43] The innervation seen post-STC is in agreement with previous studies by Frederiksen *et al.*[23,24] in rats, describing innervation arising from elongation and branching of existing nerves in the trigone. Taking this into consideration, it is reasonable to assume that nerve growth occurs in parallel to detrusor growth, and not that one precedes the other. What affect this nerve growth has on the development of other aspects of regeneration (i.e., angiogenesis) and whether all types of nerves have equal regenerative properties is also of interest and will be considered in future investigations.

To summarize, in this pilot study, we have described the early functional changes of an *in vivo* regenerating bladder without the aid of scaffold or cells and suggested the potential utility of noninvasively monitoring bladder regrowth using micro-CT measurements. Further studies are needed to evaluate the functional durability of the observed regenerative response, that is, what happens after 8 weeks post-STC. Nonetheless, our current observations indicate that despite changes in key cystometric parameters (i.e., TP/MP) as well as detrusor contractility, the bladder regeneration process invokes sufficient plasticity/accommodation to ensure maintenance of apparently normal bladder function post-STC.

Acknowledgment

This work was supported by NIH USPHS (grant no. R21DK081832). The authors thank Catherine Ward for photographic assistance during surgeries.

Disclosure Statement

No competing financial interests exist.

References

1. Roy, S., and Gatien, S. Regeneration in axolotls: a model to aim for! Exp Gerontol **43,** 968, 2008.
2. Tsonis, P.A. Bridging knowledge gaps on the long road to regeneration: classical models meet stem cell manipulation and bioengineering. Mol Interv **7,** 249, 2007.
3. Schwarz, R. Ricerche in proposito della rigenerazione della vescica urinaria. Sperimentale **45,** 484, 1891. (In Italian.)
4. Jayo, M.J., Jain, D., Wagner, B.J., and Bertram, T.A. Early cellular and stromal responses in regeneration versus repair of a mammalian bladder using autologous cell and biodegradable scaffold technologies. J Urol **180,** 392, 2008.
5. Oberpenning, F., Meng, J., Yoo, J.J., and Atala, A. *De novo* reconstitution of a functional mammalian urinary bladder by tissue engineering. Nat Biotechnol **17,** 149, 1999.
6. Liang, D.S. Secondary cystectomy in rats. J Urol **90,** 187, 1963.
7. Liang, D.S., and Goss, R.J. Regeneration of the bladder after subtotal cystectomy in rats. J Urol **89,** 427, 1963.
8. Sisk, V., and Neu, I. Regeneration of the bladder: a case study. Trans Am Assoc Genitourin Surg **32,** 197, 1939.
9. Bohne, A.W., and Urwiller, K.L. Experience with urinary bladder regeneration. J Urol **77,** 725, 1957.
10. Atala, A., Bauer, S.B., Soker, S., Yoo, J.J., and Retik, A.B. Tissue-engineered autologous bladders for patients needing cystoplasty. Lancet **367,** 1241, 2006.
11. Malmgren, A., Sjogren, C., Uvelius, B., Mattiasson, A., Andersson, K.E., and Andersson, P.O. Cystometrical evaluation of bladder instability in rats with infravesical outflow obstruction. J Urol **137,** 1291, 1987.
12. Pandita, R.K., and Andersson, K.E. Effects of intravesical administration of the K+ channel opener, ZD6169, in conscious rats with and without bladder outflow obstruction. J Urol **162,** 943, 1999.
13. Chai, T.C., Gemalmaz, H., Andersson, K.E., Tuttle, J.B., and Steers, W.D. Persistently increased voiding frequency despite relief of bladder outlet obstruction. J Urol **161,** 1689, 1999.
14. Kanematsu, A., Yamamoto, S., and Ogawa, O. Changing concepts of bladder regeneration. Int J Urol **14,** 673, 2007.
15. Kelami, A., Ludtke-Handjery, A., Korb, G., Rolle, J., Schnell, J., and Danigel, K.H. Alloplastic replacement of the urinary bladder wall with lyophilized human dura. Eur Surg Res **2,** 195, 1970.
16. Kudish, H.G. The use of polyvinyl sponge for experimental cystoplasty. J Urol **78,** 232, 1957.
17. Monsour, M.J., Mohammed, R., Gorham, S.D., French, D.A., and Scott, R. An assessment of a collagen/vicryl composite membrane to repair defects of the urinary bladder in rabbits. Urol Res **15,** 235, 1987.
18. Rohrmann, D., Albrecht, D., Hannappel, J., Gerlach, R., Schwarzkopp, G., and Lutzeyer, W. Alloplastic replacement of the urinary bladder. J Urol **156,** 2094, 1996.
19. Vaught, J.D., Kropp, B.P., Sawyer, B.D., Rippy, M.K., Badylak, S.F., Shannon, H.E., and Thor, K.B. Detrusor regeneration in the rat using porcine small intestinal submucosal grafts: functional innervation and receptor expression. J Urol **155,** 374, 1996.
20. Brooks, S.V., and Faulkner, J.A. Contraction-induced injury: recovery of skeletal muscles in young and old mice. Am J Physiol **258,** C436, 1990.
21. El-Ftesi, S., Chang, E.I., Longaker, M.T., and Gurtner, G.C. Aging and diabetes impair the neovascular potential of adipose-derived stromal cells. Plast Reconstr Surg **123,** 475, 2009.
22. Hoenig, M.R., Bianchi, C., Rosenzweig, A., and Sellke, F.W. Decreased vascular repair and neovascularization with ageing: mechanisms and clinical relevance with an emphasis on hypoxia-inducible factor-1. Curr Mol Med **8,** 754, 2008.
23. Frederiksen, H., Arner, A., Malmquist, U., Scott, R.S., and Uvelius, B. Nerve induced responses and force-velocity relations of regenerated detrusor muscle after subtotal cystectomy in the rat. Neurourol Urodyn **23,** 159, 2004.
24. Frederiksen, H., Davidsson, T., Gabella, G., and Uvelius, B. Nerve distribution in rat urinary bladder after incorporation of acellular matrix graft or subtotal cystectomy. Scand J Urol Nephrol **42,** 205, 2008.
25. Piechota, H.J., Gleason, C.A., Dahms, S.E., Dahiya, R., Nunes, L.S., Lue, T.F., and Tanagho, E.A. Bladder acellular matrix graft: *in vivo* functional properties of the regenerated rat bladder. Urol Res **27,** 206, 1999.
26. Saito, M., Yoshikawa, Y., Ohmura, M., Yokoi, K., and Kondo, A. Functional restoration of rat bladder after subtotal cystectomy: *in vivo* cystometry and *in vitro* study of whole bladder. Urol Res **24,** 171, 1996.
27. Frederiksen, H., Sjuve, R., Arner, A., and Uvelius, B. Regeneration of detrusor muscle after subtotal cystectomy in the rat: effects on contractile proteins and bladder mechanics. Neurourol Urodyn **20,** 685, 2001.

28. Biers, S.M., Reynard, J.M., Doore, T., and Brading, A.F. The functional effects of a c-kit tyrosine inhibitor on guinea-pig and human detrusor. BJU Int **97,** 612, 2006.
29. Kubota, Y., Hashitani, H., Shirasawa, N., Kojima, Y., Sasaki, S., Mabuchi, Y., Soji, T., Suzuki, H., and Kohri, K. Altered distribution of interstitial cells in the guinea pig bladder following bladder outlet obstruction. Neurourol Urodyn **27,** 330, 2008.
30. Metzger, R., Neugebauer, A., Rolle, U., Bohlig, L., and Till, H. C-Kit receptor (CD117) in the porcine urinary tract. Pediatr Surg Int **24,** 67, 2008.
31. Piotrowska, A.P., Rolle, U., Chertin, B., De Caluwe, D., Bianchi, A., and Puri, P. Alterations in smooth muscle contractile and cytoskeleton proteins and interstitial cells of Cajal in megacystis microcolon intestinal hypoperistalsis syndrome. J Pediatr Surg **38,** 749, 2003.
32. Shafik, A., El-Sibai, O., Shafik, A.A., and Shafik, I. Identification of interstitial cells of Cajal in human urinary bladder: concept of vesical pacemaker. Urology **64,** 809, 2004.
33. Galli, S.J., Zsebo, K.M., and Geissler, E.N. The kit ligand, stem cell factor. Adv Immunol **55,** 1, 1994.
34. Barile, L., Messina, E., Giacomello, A., and Marban, E. Endogenous cardiac stem cells. Prog Cardiovasc Dis **50,** 31, 2007.
35. Bearzi, C., Leri, A., Lo Monaco, F., Rota, M., Gonzalez, A., Hosoda, T., Pepe, M., Qanud, K., Ojaimi, C., Bardelli, S., D'Amario, D., D'Alessandro, D.A., Michler, R.E., Dimmeler, S., Zeiher, A.M., Urbanek, K., Hintze, T.H., Kajstura, J., and Anversa, P. Identification of a coronary vascular progenitor cell in the human heart. Proc Natl Acad Sci USA **106,** 15885, 2009.
36. Castaldo, C., Di Meglio, F., Nurzynska, D., Romano, G., Maiello, C., Bancone, C., Muller, P., Bohm, M., Cotrufo, M., and Montagnani, S. CD117-positive cells in adult human heart are localized in the subepicardium, and their activation is associated with laminin-1 and alpha6 integrin expression. Stem Cells **26,** 1723, 2008.
37. Miyamoto, S., Kawaguchi, N., Ellison, G.M., Matsuoka, R., Shin'oka, T., and Kurosawa, H. Characterization of long-term cultured c-kit+ cardiac stem cells derived from adult rat hearts. Stem Cells Dev **19,** 105, 2010.
38. Tillmanns, J., Rota, M., Hosoda, T., Misao, Y., Esposito, G., Gonzalez, A., Vitale, S., Parolin, C., Yasuzawa-Amano, S., Muraski, J., De Angelis, A., Lecapitaine, N., Siggins, R.W., Loredo, M., Bearzi, C., Bolli, R., Urbanek, K., Leri, A., Kajstura, J., and Anversa, P. Formation of large coronary arteries by cardiac progenitor cells. Proc Natl Acad Sci USA **105,** 1668, 2008.
39. Kurzrock, E.A., Lieu, D.K., Degraffenried, L.A., Chan, C.W., and Isseroff, R.R. Label-retaining cells of the bladder: candidate urothelial stem cells. Am J Physiol Renal Physiol **294,** F1415, 2008.
40. Nguyen, M.M., Lieu, D.K., deGraffenried, L.A., Isseroff, R.R., and Kurzrock, E.A. Urothelial progenitor cells: regional differences in the rat bladder. Cell Prolif **40,** 157, 2007.
41. Kaneko, H., Watanabe, H., Hosokawa, Y., Urata, Y., Hattori, T., Pellicciari, C., and Fukuda, M. The presence of G1 and G2 populations in normal epithelium of rat urinary bladder. Basic Appl Histochem **28,** 41, 1984.
42. Danzer, E., Kiddoo, D.A., Redden, R.A., Robinson, L., Radu, A., Zderic, S.A., Doolin, E.J., Adzick, N.S., and Flake, A.W. Structural and functional characterization of bladder smooth muscle in fetal rats with retinoic acid-induced myelomeningocele. Am J Physiol Renal Physiol **292,** F197, 2007.
43. Zvarova, K., and Vizzard, M.A. Distribution and fate of cocaine- and amphetamine-regulated transcript peptide (CARTp)-expressing cells in rat urinary bladder: a developmental study. J Comp Neurol **489,** 501, 2005.

Address correspondence to:
George Christ, Ph.D.
Wake Forest Institute for Regenerative Medicine
Wake Forest University School of Medicine
391 Technology Way
Winston Salem, NC 27101

E-mail: gchrist@wfubmc.edu

Received: October 22, 2009
Accepted: March 15, 2010
Online Publication Date: May 6, 2010